

# Modulation of nuclear REST by alternative splicing: a potential therapeutic target for Huntington's disease

Guo-Lin Chen<sup>a, b, c, \*</sup> , Qi Ma<sup>d</sup>, Dharmendra Goswami<sup>e, f, g</sup>, Jianyu Shang<sup>a</sup>, Gregory M. Miller<sup>a, h</sup>

<sup>a</sup> Department of Pharmaceutical Sciences and Center for Drug Discovery, School of Pharmacy, Northeastern University, Boston, MA, USA

<sup>b</sup> Guangxi Collaborative Innovation Center for Biomedicine, Guangxi Medical University, Nanning, Guangxi, China

<sup>c</sup> Research Center for Regenerative Medicine of Guangxi, Guangxi Medical University, Nanning, Guangxi, China

<sup>d</sup> Department of Psychiatry, Institute for Human Performance, SUNY Upstate Medical University, Syracuse, NY, USA

<sup>e</sup> Center for the Study of Traumatic Encephalopathy, Boston University School of Medicine, Boston, MA, USA

<sup>f</sup> Department of Neurology, Boston University School of Medicine, Boston, MA, USA

<sup>g</sup> VA Boston HealthCare System, Boston, MA, USA

<sup>h</sup> Department of Chemical Engineering, School of Engineering, Northeastern University, Boston, MA, USA

Received: October 27, 2016; Accepted: March 22, 2017

## Abstract

Huntington's disease (HD) is caused by a genetically mutated huntingtin (mHtt) protein with expanded polyQ stretch, which impairs cytosolic sequestration of the repressor element-1 silencing transcription factor (REST), resulting in excessive nuclear REST and subsequent repression of neuronal genes. We recently demonstrated that REST undergoes extensive, context-dependent alternative splicing, of which exon-3 skipping ( $\Delta E_3$ )—a common event in human and nonhuman primates—causes loss of a motif critical for REST nuclear targeting. This study aimed to determine whether  $\Delta E_3$  can be targeted to reduce nuclear REST and rescue neuronal gene expression in mouse striatal-derived, mHtt-expressing *STHdh*<sup>Q111/Q111</sup> cells—a well-established cellular model of HD. We designed two morpholino antisense oligos (ASOs) targeting the splice sites of *Rest*  $E_3$  and examined their effects on  $\Delta E_3$ , nuclear Rest accumulation and Rest-controlled gene expression in *STHdh*<sup>Q111/Q111</sup> cells. We found that (1) the ASOs treatment significantly induced  $\Delta E_3$ , reduced nuclear Rest, and rescued transcription and/or mis-splicing of specific neuronal genes (e.g. *Syn1* and *Stmn2*) in *STHdh*<sup>Q111/Q111</sup> cells; and (2) the ASOs-induced transcriptional regulation was dependent on  $\Delta E_3$  induction and mimicked by siRNA-mediated knock-down of *Rest* expression. Our findings demonstrate modulation of nuclear REST by  $\Delta E_3$  and its potential as a new therapeutic target for HD and provide new insights into environmental regulation of genome function and pathogenesis of HD. As  $\Delta E_3$  is modulated by cellular signalling and linked to various types of cancer, we anticipate that  $\Delta E_3$  contributes to environmentally tuned REST function and may have a broad range of clinical implications.

**Keywords:** REST/NRSF • alternative splicing • nuclear translocation • gene therapy • Huntington's disease • antisense oligos • Syn-1 • Stmn2 • PPAR $\gamma$

## Introduction

Originally identified as a transcriptional repressor of neuronal genes, the repressor element-1 silencing transcription factor (REST, also named NRSF for neuron-restrictive silencing factor) is now recognized as a coordinate transcriptional and epigenetic regulator that orchestrates cellular epigenome [1,2]. REST contains a DNA-binding domain consisting of eight zinc fingers (ZFs), which is sandwiched by

two repression domains capable of recruiting numerous transcriptional and epigenetic cofactors, through which REST promotes dynamic, context-dependent chromatin remodelling and repression or activation of thousands of genes [2,3]. As such, REST controls many cellular processes fundamental to normal physiology and pathological conditions and is implicated in a wide range of human diseases including cancer and neurodegenerative diseases.

The physical separation of the genome from cytoplasm by nuclear envelope in eukaryotic cells requires translocation of REST from cytoplasm to nucleus to modulate genome function. It was documented

\*Correspondence to: Dr. Guo-Lin CHEN  
E-mail: chen\_guolin@hotmail.com

doi: 10.1111/jcmm.13209

that ZF-5 is critical for REST nuclear targeting [4,5] and that altered nuclear REST is implicated in adenovirus-induced cell transformation [6], ageing and neurodegenerative diseases including Huntington's and Alzheimer's diseases (HD and AD) [7,8]. Notably, a protein named huntingtin (Htt) associates with REST through a cytoskeletal complex which prevents nuclear translocation of REST; however, Htt is mutated in HD, leading to impaired cytosolic sequestration of REST and excessive accumulation of nuclear REST, which in turn represses neuronal genes important for the maintenance and function of specific neurons [8–10]. Accordingly, rescue of neuronal gene expression through modulation of REST activity has been suggested as a therapeutic strategy for HD [11,12].

As a multi-exonic gene, *REST* undergoes alternative splicing, a cotranscriptional process which enables a single gene to produce multiple mRNA and protein variants, with an N-terminal REST4 isoform having been well documented [8,13]. Recently, we identified 45 *REST* mRNA splice variants with highly context-dependent expression, suggesting an underappreciated role of alternative splicing in modulation of REST function [14]. Particularly, skipping of exon-3 ( $\Delta E_3$ ), a common splicing event which eliminates ZF-5 critical for REST nuclear targeting, is linked to cancer and modulated by pioglitazone—a highly selective activator of the peroxisome proliferator-activated receptor gamma (PPAR $\gamma$ ) exerting biological actions overlapping with REST [15–17]. Hence, we suggested that  $\Delta E_3$  may act as an endogenous, manipulable modulator of REST activity, and it may be targeted to treat HD related to REST dysfunction.

To test this hypothesis, we determined whether manipulation of  $\Delta E_3$  alters nuclear REST and neuronal gene expression in a cell model of HD. We designed two antisense oligos (ASOs) targeting the splice sites of *Rest*  $E_3$  and examined their effects on  $\Delta E_3$ , nuclear Rest and neuronal gene expression in STHdh<sup>Q111/Q111</sup> cells. We demonstrated that treatment of STHdh<sup>Q111/Q111</sup> cells with the ASOs significantly induced  $\Delta E_3$ , reduced nuclear Rest and rescued transcription and/or mis-splicing of specific neuronal genes and that the ASOs-induced transcriptional regulation was dependent on  $\Delta E_3$  induction while mimicked by siRNA knock-down of Rest. Our findings validate  $\Delta E_3$  as a modulator of nuclear REST and a potential therapeutic target for HD and provide new insights into HD pathogenesis.

## Materials and methods

### Cell culture and treatment

STHdh<sup>Q77</sup> and STHdh<sup>Q111/Q111</sup> cells (Coriell Institute, Camden, NJ, USA) were cultured in advanced DMEM (Invitrogen, Carlsbad, CA, USA) supplemented with 10% heat-inactivated FBS, 1% penicillin/streptomycin and 200  $\mu$ g/ml G418 (Invitrogen) at 33°C in a 5% CO<sub>2</sub> incubator. The two cell lines were established from knock-in transgenic mice containing humanized *Htt* exon 1 with seven and 111 polyQ repeats, respectively, of which STHdh<sup>Q111/Q111</sup> is a well-established cell model of HD [18–21]. Passages 3–9 of the cells were used for all experiments.

For ASOs treatment, 3  $\mu$ M of morpholino ASOs ( $I_2E_3$  and  $E_3I_3$ , alone or combined) or a control oligo (Gene Tools, Philomath, OR, USA) were delivered into cells using 6  $\mu$ M of Endo-Porter (Gene Tools). For RNAi

experiment, 10 nM of 27mer Rest (mouse) siRNAs (siRNA-1 and -2) or a negative siRNA (OriGene, Rockville, MD, USA) were transfected into cells using siTran 1.0 Transfection Reagent (OriGene). Cells were harvested for various analyses at 48 hrs post-treatment, and experiments were performed in duplicate on three independent occasions.

### Immunofluorescence confocal microscopy and image analysis

Two widely used anti-REST antibodies, sc-25398 (Santa Cruz, Dallas, TX, USA) and ab21635 (Abcam, Cambridge, MA, USA), were employed to perform immunocytochemistry (ICC). Briefly, cells cultured on poly-D-lysine-coated coverslips were treated with ASOs ( $I_2E_3$  +  $E_3I_3$ ) or a control oligo. After 48-hr incubation, cells were fixed with 4% paraformaldehyde, permeabilized with 0.3% Triton X-100 and incubated with sc-25398 (1:100) or ab21635 (1:200), followed by incubation with a goat anti-rabbit secondary antibody conjugated with Alexa dye (1:500; Invitrogen). Nuclei were stained with Hoechst-33342 (Thermo Scientific, Waltham, MA, USA), and cells were mounted on glass slides.

For confocal microscopy, image stacks along the z-axis were acquired using a Leica TCS SP5 Spectral Confocal Microscope (Leica Microsystems, Cambridge, UK). Image acquisition settings were kept the same for all scans in the same experiment group when fluorescence intensity was compared. Images were analysed using ImageJ program (NIH). Fluorescence intensities measured as integrated pixel intensities were determined for the entire cell and its nucleus area, respectively. Nucleus percentage of fluorescence intensity was calculated for each cell, and values of 100 cells in each group were averaged and presented as Mean  $\pm$  S.E.M. All groups to be compared were run simultaneously using cells from the same culture preparations.

### RNA isolation and cDNA synthesis

Total RNA was extracted using Trizol<sup>®</sup> reagent (Invitrogen) and reverse transcribed into cDNA using Superscript<sup>™</sup> III reverse transcriptase and oligo-dTs (Invitrogen). To avoid DNA contamination, samples were treated with RQ1 RNase-free DNase I (Promega, Madison, WI, USA) for 1 hr at 37°C. Synthesized cDNA was diluted to 50 ng/ $\mu$ l for use.

### Polymerase chain reaction (PCR)

For detection of  $\Delta E_3$ , nested PCR was performed as previously described [14] in a MJ Research PTC-200 Peltier Thermal Cycler using Rest- $E_1F_2/E_4R_3$  and Rest- $E_2F_2/E_4R_1$  (or - $E_1F_1/E_4R_1$ ) (Table 1) as the primer set for 1st- and 2nd-round amplification, respectively. PCR with Syn1- $E_7F_1/E_9R_1$  was performed to verify Syn1 variants with/-out intron-8 ( $I_8$ ). PCR products were electrophoresed on 2% agarose gel, excised, purified and sequence verified. DNA sequencing was serviced by Functional Biosciences (Madison, WI, USA).

### Quantitative real-time PCR (qRT-PCR)

SYBR Green qRT-PCR for *Bdnf*, *Stmn2*, *Syn1*, *Gapdh*, *Nmnat2*, *Lrp11*, *Rtn2* and specific *Rest* variants was performed using primers listed in

**Table 1** Oligos used for PCR,  $\Delta E_3$  manipulation and RNAi

| Name                                 | Sequence (5' to 3')       | Note  |
|--------------------------------------|---------------------------|---|
| <i>Regular PCR</i>                   |                           |   |
| Rest-E <sub>1</sub> F <sub>2</sub>   | CCTCGACGCCCAACTTTTCC      |   |
| Rest-E <sub>4</sub> R <sub>3</sub>   | CACATAATTGCACTGATCACATTTA |   |
| Rest-E <sub>1</sub> F <sub>1</sub>   | CGAAACTCCAGCAACAAAGA      |   |
| Rest-E <sub>2</sub> F <sub>2</sub>   | CACCTGCAGCAAGTGAACACTACT  |   |
| Rest-E <sub>4</sub> R <sub>1</sub>   | CTGCACTGATCACATTTAAATG    |   |
| Syn1-E <sub>7</sub> F <sub>1</sub>   | CTGAGCCCTTCATTGATGCT      |   |
| Syn1-E <sub>9</sub> R <sub>1</sub>   | CACTGCGCAGATGTCAAGTC      |   |
| <i>qRT-PCR (SYBR Green I)</i>        |                           |   |
| Rest-E <sub>2/4</sub> F <sub>1</sub> | ACCACTGGAGGAAACACCTG      | For E <sub>2</sub> /E <sub>4</sub> ( $\Delta E_3$ ) variant |
| Rest-E <sub>2/4</sub> R <sub>1</sub> | TTTAAATGGCTTCTCACCTGTG    |   |
| Rest-E <sub>3</sub> F <sub>1</sub>   | AACTCATACAGGAGAAGCCCC     | Paired with Rest-E <sub>4</sub> R <sub>1</sub>              |
| Syn1-E <sub>8</sub> F <sub>1</sub>   | GAGCAGATTGCCATGTCTGA      | Paired with Syn1-E <sub>9</sub> R <sub>1</sub>              |
| Syn1-E <sub>3</sub> F <sub>1</sub>   | GCCAATGGTGGATTCTCTGT      | For global Syn1   |
| Syn1-E <sub>4</sub> R <sub>1</sub>   | CAGCCCAATGACCAAACCTC      |   |
| Syn1-E <sub>8</sub> F <sub>2</sub>   | TGTCGGGTAAGTGAAGACC       | For E <sub>8</sub> /I <sub>8</sub> /E <sub>9</sub> variant  |
| Syn1-I <sub>8</sub> R <sub>1</sub>   | GCTGTGCTTCTGCTCTCA        |   |
| Bdnf-F <sub>1</sub>                  | TCGTTCCCTTCGAGTTAGCC      |   |
| Bdnf-R <sub>1</sub>                  | TTGGTAAACGGCACAACAAACA    |   |
| Stmn2-F <sub>1</sub>                 | GCAATGGCCTACAAGGAAAA      |   |
| Stmn2-R <sub>1</sub>                 | GGTGGCTTCAAGATCAGCTC      |   |
| Gapdh-F <sub>3</sub>                 | GAACGGATTGGCCGTATCGG      |   |
| Gapdh-R <sub>3</sub>                 | TCGCTCCTGGAAGATGGTGAT     |   |
| Rtn2-F <sub>1</sub>                  | GACTCGGGAGCAGACAGAAC      |   |
| Rtn2-R <sub>1</sub>                  | TGACAAGAGTCAAGCCGTTG      |   |
| Lrp11-F <sub>1</sub>                 | AGCCACTACCCACAACCAAC      |   |
| Lrp11-R <sub>1</sub>                 | AAAACAGTGATGGCCAGACC      |   |
| Nmnat2-F <sub>1</sub>                | ACCCATGGGAGTGCTATCAG      |   |
| Nmnat2-R <sub>1</sub>                | CAGGTGTCATGGAAGGTGTG      |   |
| <i>Morpholino oligos</i>             |                           |   |
| I <sub>2</sub> E <sub>3</sub>        | GGCGTTCTCCTGCAAAGTCATAAT  |   |
| E <sub>3</sub> I <sub>3</sub>        | GCAGTCACCATCTTACCAACCTGAA |   |

**Table 1.** Continued

| Name                             | Sequence (5' to 3')                            | Note                             |
|----------------------------------|--|----------------------------------|
| Control                          | CCTCTTACCTCAGTTACAATTATA                       |                                  |
| <i>Trilencer-27 siRNA duplex</i> |  |                                  |
| siRNA-1                          | rCrCrCrGrUrArUrArArUrGrUrGrArArCrUrUrUrGrUrCCT | Target <i>Rest E<sub>3</sub></i> |
| siRNA-2                          | rArGrGrArCrArGrArUrUrGrUrArArCrUrArGrCrUrCrGTG | Target <i>Rest 3'-UTR</i>        |

PCR, polymerase chain reaction. (1) Rest-E<sub>1</sub>F<sub>2</sub> paired with -E<sub>4</sub>R<sub>3</sub> were used for 1st round of nested PCR, while REST-E<sub>4</sub>R<sub>1</sub> paired with -E<sub>1</sub>F<sub>1</sub> or -E<sub>2</sub>F<sub>2</sub> were used for 2nd round of nested PCR; (2) Syn1-E<sub>7</sub>F<sub>1</sub> paired with -E<sub>9</sub>R<sub>1</sub> were used for verification of I<sub>8</sub> retention in mRNA.

Table 1 in a Roche LightCycler 2.0 system (Roche Diagnostics, Indianapolis, IN, USA) as previously described [14]. The unique amplicon was verified for each assay, and the threshold cycle (C<sub>t</sub>) values were used to evaluate expression change between groups using the 2<sup>- $\Delta\Delta C_t$</sup>  approach [22] with *Gapdh* as the reference.

## Transcriptional profiling

Three total RNA samples of high quality (RNA integrity number: 8.6–9.4) isolated from cells treated with ASOs (I<sub>2</sub>E<sub>3</sub> + E<sub>3</sub>I<sub>3</sub>) (Q111-ASOs) or a control oligo (Q111- and Q7-Control) were transcriptionally profiled by the Affymetrix's GeneChip<sup>®</sup> Mouse Gene 2.0 ST Array serviced by EpigenDx (Hopkinton, MA, USA). Pairwise comparisons of expression between the samples were performed by analysis of variance (ANOVA) using the Partek<sup>®</sup> Genomic Suite<sup>®</sup> software (St. Louis, MO, USA). The heat map was generated by hierarchical clustering of expression values using the genes generated by ANOVA comparisons between the samples. The mean expression is shifted to 0 and scaled to a S.D. of 1.

## Western blotting for Stmn2

Cytoplasmic protein fraction was extracted using NE-PER<sup>®</sup> Nuclear and Cytoplasmic extraction reagents (Thermo Scientific), and protein concentration was determined by Bradford assay. The same amount (40  $\mu$ g) of protein was boiled with 2 $\times$  Laemmli buffer, electrophoresed on a 10% SDS-PAGE gel and electrotranslocated onto an Immun-Blot PVDF membrane (Bio-Rad, Hercules, CA, USA) presoaked in methanol. The membrane was blocked with 5% non-fat milk and incubated with a goat anti-STMN2 (SAB2500997) (Sigma-Aldrich, St Louis, MO, USA) at 1:500 overnight at 4°C, followed by incubation with a rabbit anti-goat IgG (A5420; Sigma-Aldrich) at 1:2500 for 1 hr at room temperature. Gapdh was blotted as a loading control using a mouse anti-GAPDH (TA802519; OriGene) and a rabbit antimouse IgG (A9044; Sigma-Aldrich). Immunoreactive signals were detected using the VisiGlo<sup>™</sup> Select HRP Chemiluminescent Substrate Kit (Amresco, Solon, OH, USA) with an ECL-based LAS-3000 image system (Fujifilm, Life Science, New Haven, CT, USA). Densitometric analysis was carried out using Image-Gauge (Fujifilm). Assays were performed on three independent occasions.

## ELISA for Bdnf

Cells were lysed using the lysis buffer consisting of 10% glycerol, 25 mM Tris-HCl (pH 7.5), 150 mM NaCl, 1% Triton X-100, 5 mM EDTA and 1 mM EGTA supplemented with 1:100 Halt™ Protease Inhibitor cocktail (Thermo Scientific). Samples were homogenized, sonicated and centrifuged at maximum speed for 10 min. at 4°C, and the supernatants were collected and stored at -80°C. Samples were assayed using a mouse Bdnf ELISA Kit (Boster, Fremont, CA, USA). Assays were performed in triple on three independent occasions.

## Bioinformatics and data analysis

Bioinformatics were performed by checking specific tracks provided by the UCSC Genome Browser (<http://genome.ucsc.edu>). Statistics were carried out using the SAS Software Version 9.4 (SAS Institute Inc., Cary, NC, USA). Comparisons of nuclear REST percentage and mRNA/protein expression level between different groups were performed by appropriate ANOVA or Student's *t*-test.

## Results

### Induction of $\Delta E_3$ by ASOs targeting the splice sites of $E_3$

We designed two ASOs ( $I_2E_3$  and  $E_3I_3$ , Fig. 1A) targeting the splice acceptor and donor sites of *Rest*  $E_3$ , respectively. As shown in Figure 1B, both ASOs induced  $\Delta E_3$  in  $STHdh^{Q7/Q7}$  and  $STHdh^{Q111/Q111}$  cells, as indicated by formation and up-regulation of the  $E_2/E_4$  ( $\Delta E_3$ ) and  $E_1/E_4$  ( $\Delta E_2 + \Delta E_3$ ) variants, respectively, as well as apparent reduction of  $E_3$ -retained variants ( $E_2/E_3/E_4$  and  $E_1/E_3/E_4$ ). In both  $STHdh^{Q7/Q7}$  and  $STHdh^{Q111/Q111}$  cells, based on the ratio of variants with/out  $\Delta E_3$ ,  $E_3I_3$  induced more  $\Delta E_3$  than  $I_2E_3$ , while combination of the two ASOs yielded the most  $\Delta E_3$  induction, such is validated by qRT-PCR-assayed expression of the  $E_2/E_4$  variant (Fig. 1C) using primer set *Rest-E<sub>2/4</sub>F<sub>1</sub>/R<sub>1</sub>* listed in Table 1. The ASOs also induced  $\Delta E_3$  in mouse primary hippocampal neurons (implying a potential *in vivo* effect), along with cells of other species including human NCCIT and rat RN46A cells (Fig. S1A), which may be explained by the highly conserved intron–exon junctions of  $E_3$  as indicated by the 'Vertebrate Multiz Alignment & Conservation' track from the UCSC Genome Browser (data not shown).

### ASOs-induced reduction of nuclear Rest in $STHdh^{Q111/Q111}$ cells

To examine whether the ASOs reduced nuclear Rest in  $STHdh^{Q111/Q111}$  cells, we performed ICC with two antibodies (sc-25398 and ab21635) against the N- and C-terminal of REST, respectively. As shown in Figure 2 and Figure S2, regardless of the antibody, accumulation of nuclear Rest was significantly higher in  $STHdh^{Q111/Q111}$  than that in  $STHdh^{Q7/Q7}$ , while ASOs treatment ( $I_2E_3 + E_3I_3$ ) significantly reduced

nuclear Rest in  $STHdh^{Q111/Q111}$  cells. ASOs-induced reduction in nuclear Rest was also observed in RN46A as indicated by ICC (Fig. S1B).

### ASOs-induced transcriptional derepression of Rest target genes in $STHdh^{Q111/Q111}$ cells

We then determined the effect of ASOs treatment on transcription of three well-documented REST target genes, *Bdnf*, *Syn1* and *Stmn2* (also named *Scg10*), in  $STHdh^{Q111/Q111}$  cells. To evaluate the relevance of ASOs-induced transcriptional regulation to altered Rest activity, we also examined regulation of the genes by two *Rest* siRNAs. As shown in Figure 3A, we found that (1) transcription of the three genes (especially *Stmn2*) was repressed in  $STHdh^{Q111/Q111}$  compared with  $STHdh^{Q7/Q7}$ ; (2) the ASOs treatment increased transcription of the genes depending on  $\Delta E_3$  induction ( $I_2E_3 < E_3I_3 < I_2E_3 + E_3I_3$ ); that is,  $\Delta E_3$  exerts a dose-dependent rescue of gene transcription; (3) ASOs-induced transcriptional regulation was mimicked by two different siRNAs which reduced Rest mRNA expression by ~70% as assayed by qRT-PCR with *Rest-E<sub>3</sub>F<sub>1</sub>/E<sub>4</sub>R<sub>1</sub>*; and (4) compared with *Bdnf*, *Stmn2* and *Syn1* showed greater repression in  $STHdh^{Q111/Q111}$  and more derepression by ASOs/siRNAs.

Unexpectedly, we identified a new *Syn1* splice variant (*Syn1-S*, GenBank Accession No. KJ174470) with  $I_8$  retention during verification of qRT-PCR product for *Syn1-E<sub>8</sub>F<sub>1</sub>/E<sub>9</sub>R<sub>1</sub>*. As shown in Figure 3B and C, we found that *Syn1-S* was abundantly expressed in  $STHdh^{Q111/Q111}$  but barely in  $STHdh^{Q7/Q7}$ , while its expression in  $STHdh^{Q111/Q111}$  was decreased by ASOs treatment in relation to  $\Delta E_3$  induction and that the ASOs-induced rescue of *Syn1* mis-splicing was mimicked by *Rest* siRNAs. Notably,  $I_8$  retention is predicted to introduce a pre-mature stop codon and therefore predictive of a truncated N-terminal *Syn1-S* protein isoform missing partial domains and phosphorylation sites.

To determine whether additional genes were transcriptionally derepressed by the ASOs, we performed gene expression array to compare global transcription between three representative samples (Q111-Control, Q111-ASOs and Q7-Control; GEO Accession No. GSE77194). As shown in Figure 3D and Table 2, global transcription differed significantly between  $STHdh^{Q7/Q7}$  and  $STHdh^{Q111/Q111}$  cells, while repression of numerous genes in  $STHdh^{Q111/Q111}$  was derepressed, at least in part, by ASOs treatment ( $I_2E_3 + E_3I_3$ ). With a two-fold change as the criteria for significance, the transcriptional data well supported the qRT-PCR assayed *Stmn2* and *Syn1* expression change and extended ASOs-induced transcriptional derepression to another 15 genes (*Sarm1*, *Nmnat2*, *Kcnk3*, *Stmn3*, *Gnptg*, *H2-T23*, *Ppm1e*, *Fbxl16*, *Lrp11*, *Ina*, *Gdap1 I1*, *Unc13a*, *Vgf*, *Rundc3a* and *Rtn2*), of which *Nmnat2*, *Lrp11* and *Rtn2* were selectively confirmed by qRT-PCR with additional samples (data not shown).

### ASOs-induced protein expression change of Rest target genes in $STHdh^{Q111/Q111}$ cells

We also performed Western blotting and ELISA to evaluate ASOs-induced regulation of *Stmn2* and *Bdnf* protein expression,

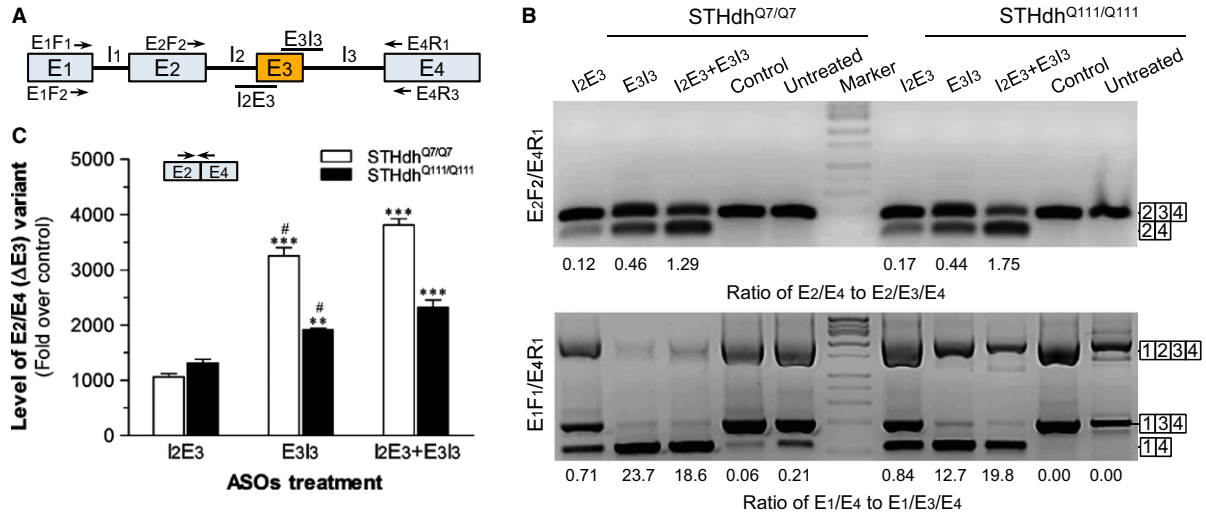


**Fig. 1** Induction of *Rest*  $\Delta E_3$  by specific ASOs in STHdh<sup>Q7/Q7</sup> and STHdh<sup>Q111/Q111</sup> cells. **(A)** Schematic structure of *Rest* gene and targeted splicing sites of the two ASOs (l<sub>2</sub>E<sub>3</sub> and E<sub>3</sub>l<sub>3</sub>). Primers used for polymerase chain reaction (PCR) detection of  $\Delta E_3$  are shown by arrows. **(B)** PCR verification of ASOs-induced  $\Delta E_3$ . Cells treated with the ASOs (l<sub>2</sub>E<sub>3</sub> and/or E<sub>3</sub>l<sub>3</sub>, 3  $\mu$ M of each) or a control oligo were harvested for RNA isolation at 48 hrs post-treatment. Nested PCR was performed with E<sub>1</sub>F<sub>1</sub>/E<sub>4</sub>R<sub>3</sub> and E<sub>2</sub>F<sub>2</sub>/E<sub>4</sub>R<sub>1</sub> (or E<sub>1</sub>F<sub>1</sub>/E<sub>4</sub>R<sub>1</sub>) as the primer set for the 1st- and 2nd-round amplification, respectively. Amplicons were sequence verified, and ratio of the variants with/without  $\Delta E_3$  for each lane was analysed by GeneTools software (Syngene, Cambridge, UK). **(C)** Relative expression of the E<sub>2</sub>/E<sub>4</sub> ( $\Delta E_3$ ) mRNA assayed by qRT-PCR with E<sub>2</sub>/E<sub>4</sub>F<sub>1</sub>/R<sub>1</sub>. The E<sub>2</sub>/E<sub>4</sub> mRNA levels were expressed as folds over the control using *Gapdh* as the reference. Data are shown as Mean  $\pm$  S.E.M. ANOVA:  $F = 165.54$ ,  $P < 0.0001$  for STHdh<sup>Q7/Q7</sup>;  $F = 32.76$ ,  $P = 0.0006$  for STHdh<sup>Q111/Q111</sup>.  $^{***}P < 0.01$ ,  $^{***}P < 0.001$  compared with l<sub>2</sub>E<sub>3</sub> group;  $^{\#}P < 0.05$  compared with l<sub>2</sub>E<sub>3</sub> + E<sub>3</sub>l<sub>3</sub> group.

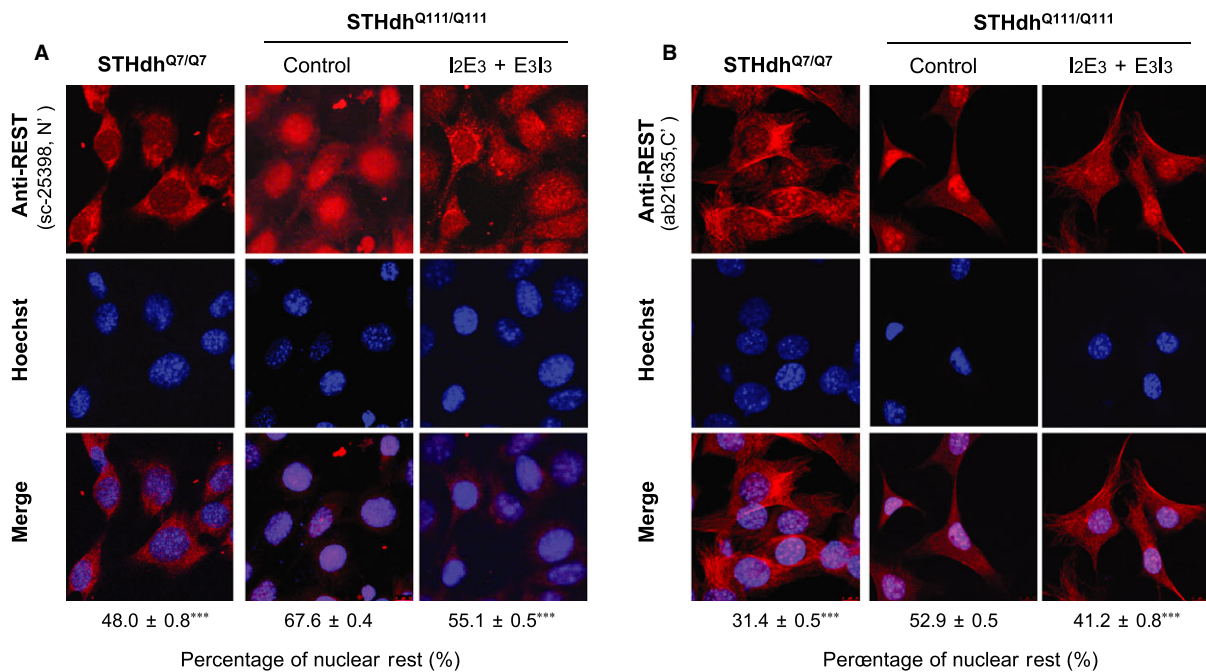


**Fig. 2** Immunofluorescence analysis of STHdh<sup>Q7/Q7</sup> and STHdh<sup>Q111/Q111</sup> cells with or without ASOs treatment. ICC was performed on with P3 and P6 cells using the antibody sc-25398 **(A)** and ab21635 **(B)** against N- and C-terminal of REST, respectively. Note that the two ASOs were combined for the treatment. Percentage of nuclear REST was analysed by ImageJ, and values of 100 cells were averaged for each group and shown as Mean  $\pm$  S.E.M.  $^{***}P < 0.001$  compared with the control STHdh<sup>Q111/Q111</sup> group by Student's *t*-test.

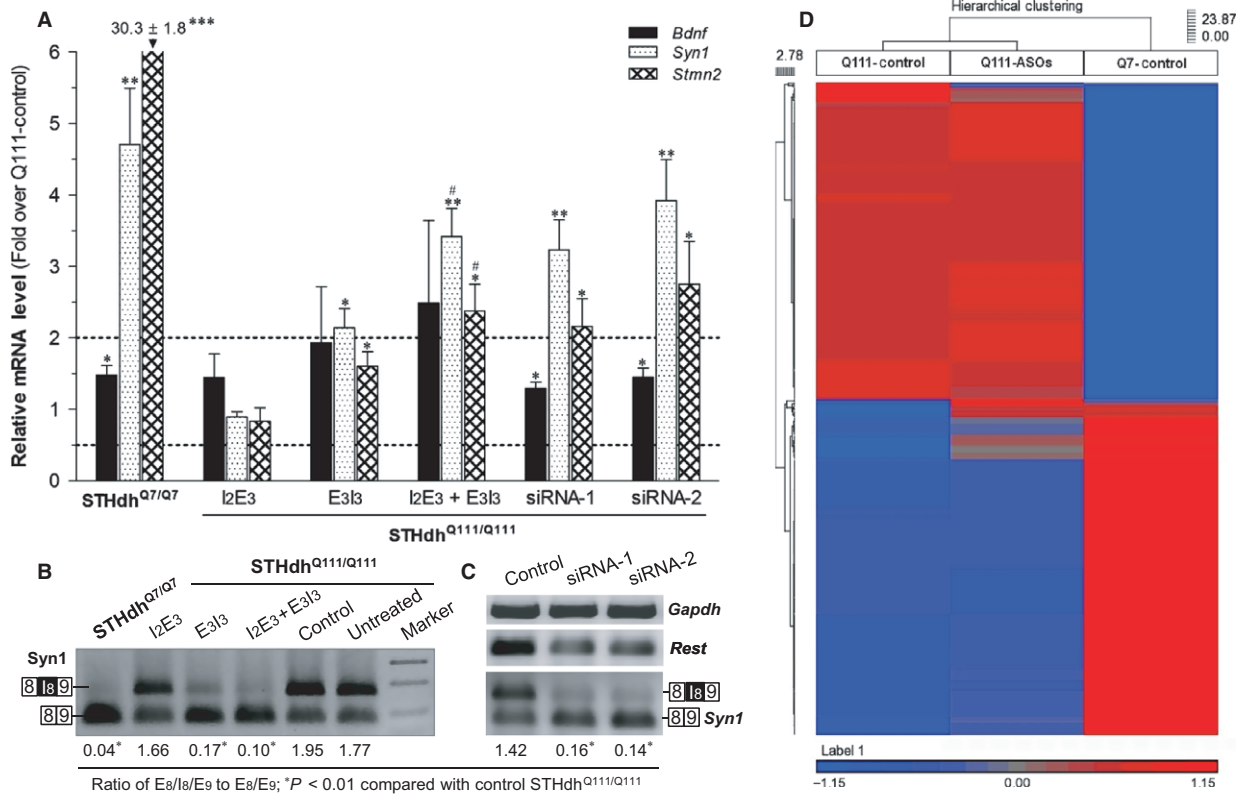


**Fig. 3** Comparison of REST-controlled gene transcription between STHdh<sup>Q7/Q7</sup> and STHdh<sup>Q111/Q111</sup> cells with or without ASOs and siRNA treatment. **(A)** Transcriptional regulation of *Bdnf*, *Syn1* and *Stmn2* by ASOs and siRNAs. qRT-PCR-assayed mRNA levels of the genes were expressed as fold over the control STHdh<sup>Q111/Q111</sup> and shown as Mean±SEM (n = 3). \*P < 0.05, \*\*P < 0.01, \*\*\*P < 0.001 compared with STHdh<sup>Q111/Q111</sup> treated with a control oligo or non-specific siRNA; #P < 0.05 compared with the E<sub>3</sub>l<sub>3</sub> group. **(B)** Syn1 mis-splicing of in STHdh<sup>Q7/Q7</sup> and STHdh<sup>Q111/Q111</sup> cells with/-out ASOs treatment. **(C)** Rescue of Syn1 mis-splicing by Rest siRNAs. Note that amplicons shown for **(B)** and **(C)** were products of qRT-PCR with Syn1-E<sub>8</sub>F<sub>1</sub>/E<sub>9</sub>R<sub>1</sub>, Rest-E<sub>3</sub>F<sub>1</sub>/E<sub>4</sub>R<sub>1</sub> and Gapdh-F<sub>3</sub>/R<sub>3</sub>. Ratio of the two Syn1 variants with/-out I<sub>8</sub> was assessed by GeneTools software (Syngene) and averaged for three occasions. **(D)** Comparison of transcriptome between STHdh<sup>Q7/Q7</sup> and STHdh<sup>Q111/Q111</sup> with/-out ASOs treatment. Three RNA samples (Q111-Control, Q111-ASOs and Q7-Control) were transcriptionally profiled, and hierarchical clustering analysis of expression values was carried out using the genes generated by ANOVA comparisons between the samples.

respectively. As shown in Figure 4A and B, compared with STHdh<sup>Q7/Q7</sup>, STHdh<sup>Q111/Q111</sup> expressed significantly lower levels of *Stmn2* and BDNF, of which *Stmn2* protein expression was significantly increased by ASOs treatment (l<sub>2</sub>E<sub>3</sub> + E<sub>3</sub>l<sub>3</sub>), while there is a tendency for the BDNF protein expression to be increased by the ASOs.

## Discussion

As a major orchestrator of the cellular epigenome, REST governs the dynamic, context-dependent expression of a huge gene network; however, it is poorly understood how REST function is environmentally tuned to moderate the dynamic, context-dependent genome function. Emerging evidence indicates that *pre*-mRNA splicing is environmentally regulated through epigenetic mechanisms [23,24], suggesting a role of alternative splicing in environmentally tuned genome function fundamental to all aspects of cellular processes. In support

of this notion, a shift from the full-length REST to a truncated REST<sub>4</sub>, which is caused by inclusion of an extra exon (N<sub>3c</sub>) introducing a premature stop codon, contributes to neurogenesis—a process for neural stem/progenitor cells to differentiate into neurons [25]. Recently, we demonstrated that *REST* undergoes extensive, context-dependent alternative splicing, suggesting a major role of alternative splicing in environmental modulation of REST function; however, functionalities of most splicing events and mRNA variants are yet to be determined albeit somewhat predictable. Using specific ASOs and a cellular model of HD, our present study validates mechanism by which a common splicing (ΔE<sub>3</sub>) modulates REST activity, as well as its potential as a therapeutic target for HD—a neurodegenerative disease associated with excessive nuclear REST.

ASOs are widely used for study of alternative splicing and may be utilized for gene therapy [26–28]. Just as expected, the two ASOs targeting *Rest* E<sub>3</sub> significantly induced ΔE<sub>3</sub>, reduced nuclear Rest and rescued neuronal gene expression in a cellular model of HD, while the

**Table 2** Genes with more than twofold change in transcription induced by both mHtt and ASOs

| Symbol          | Fold change |           | Gene function   |
|-----------------|-------------|-----------|---|
|                 | Q7/Q111     | ASOs/Ctrl |   |
| <i>Sarm1</i>    | 2.1         | 2.2       | Negative regulator of MYD88/TRIF-dependent Toll-like receptor signalling pathway which plays a pivotal role in activating axonal degeneration following injury; Also involved in immune response. |
| <i>Nmnat2</i>   | 6.3         | 2.2       | Catalyses an essential step in NAD (NADP) biosynthetic pathway  |
| <i>Kcnk3</i>    | 4.0         | 2.2       | An outwardly rectifying channel sensitive to changes in extracellular pH  |
| <i>Stmn2</i>    | 27.3        | 2.2       | A member of the stathmin family of phosphoproteins; Regulator of microtubule stability and neuronal growth.   |
| <i>Gnptg</i>    | 2.3         | 2.3       | Catalyses the first step in synthesis of a mannose 6-phosphate lysosomal recognition marker; Necessary for targeting of lysosomal hydrolases to the lysosome.                                     |
| <i>Stmn3</i>    | 7.4         | 2.3       | A member of the stathmin protein family which form a complex with tubulins; Involved in microtubule formation and function.   |
| <i>H2-T23</i>   | 2.3         | 2.3       | Involved in immune response   |
| <i>Ppm1e</i>    | 3.9         | 2.4       | Dephosphorylates and inactivates multiple substrates including serine/threonine-protein kinase 1, AMPK and the multifunctional calcium/calmodulin-dependent protein kinases                       |
| <i>Fbxl16</i>   | 3.9         | 2.5       | Functions in protein ubiquitination   |
| <i>Gdap1 11</i> | 4.1         | 2.7       | Likely functions in neuron differentiation; Associated with neuroblastoma.  |
| <i>Syn1</i>     | 6.7         | 3.0       | Plays a role in regulation of axonogenesis, synaptogenesis and neurotransmitter release   |
| <i>Ina</i>      | 2.4         | 3.1       | Facilitates axonal neurite elongation in neuroblastoma cells; Involved in morphogenesis of neurons  |
| <i>Lrp11</i>    | 3.2         | 3.5       | Involved in multicellular organismal response to stress   |
| <i>Unc13a</i>   | 6.8         | 3.6       | Binds to phorbol esters and diacylglycerol; Plays a role in neurotransmitter release at synapses  |
| <i>Vgf</i>      | 6.4         | 3.7       | Plays a role in maintenance of organismal energy balance and hippocampal synaptic activity  |
| <i>Rundc3a</i>  | 9.3         | 3.9       | Regulator of guanylate cyclase activity   |
| <i>Rtn2</i>     | 10.0        | 6.1       | Plays a role in generation of tubular endoplasmic reticulum and intracellular vesicular transport   |

Q7/Q111—relative mRNA expression in  $STHdh^{Q7/Q7}$  over  $STHdh^{Q111/Q111}$  (both were treated with a control oligo). ASOs/Ctrl—relative mRNA expression in ASOs-treated  $STHdh^{Q111/Q111}$  over control  $STHdh^{Q111/Q111}$ .

ASOs-induced transcriptional regulation was mimicked by siRNAs which considerably down-regulate *Rest* mRNA expression, suggesting a causative link from ASOs-induced  $\Delta E_3$  to Rest activity. As  $\Delta E_3$  does not occur naturally in rodents, our findings were unlikely confounded by endogenous  $\Delta E_3$ . So, as illustrated in Figure 5, this study provides evidence for  $\Delta E_3$  as an endogenous modulator of REST activity as well as a potential therapeutic avenue for HD. As  $\Delta E_3$  is modulated by pioglitazone [14]—a highly selective PPAR $\gamma$  activator clinically used for type 2 diabetes but reportedly associated with increased risk of bladder cancer [29], it is possible that  $\Delta E_3$  contributes, at least in part, to pharmacological actions of PPAR $\gamma$  and may thus have been inadvertently targeted for disease therapy. However, mechanisms involved in PPAR $\gamma$  regulation of gene expression are rather complex, and coinciding with the absence of natural  $\Delta E_3$  in rodents, pioglitazone exerts no effect on  $\Delta E_3$  in  $STHdh^{Q111/Q111}$  cells (data not shown), such that PPAR $\gamma$  ligands (*e.g.* pioglitazone) are not

suitable for the study of  $\Delta E_3$ . As REST controls many cellular processes fundamental to normal physiology and disease aetiology,  $\Delta E_3$  manipulation may have a broad range of clinical implications (*e.g.* cancer therapy and stem cell engineering). Notably, while the ASOs induced  $\Delta E_3$  in both  $STHdh^{Q7/Q7}$  and  $STHdh^{Q111/Q111}$  cells, their effects on nuclear REST and gene transcription were only pronounced in  $STHdh^{Q111/Q111}$  but not in  $STHdh^{Q7/Q7}$  cells (data not shown), presumably due to a low level of basal nuclear Rest maintained by the normal nucleocytoplasmic shuttling in  $STHdh^{Q7/Q7}$  cells. Also, it should be pointed out that although both  $\Delta E_3$  induction and RNAi down-regulate Rest function, their effects are mediated by different mechanisms. While RNAi reduces globe expression of Rest isoforms including the full-length Rest,  $\Delta E_3$  induction does not affect total Rest expression but alters ratio of two types Rest isoforms discriminated by the capability of being transported into nucleus. Hence, a specific Rest isoform (*e.g.* the full-length Rest) might be differentially

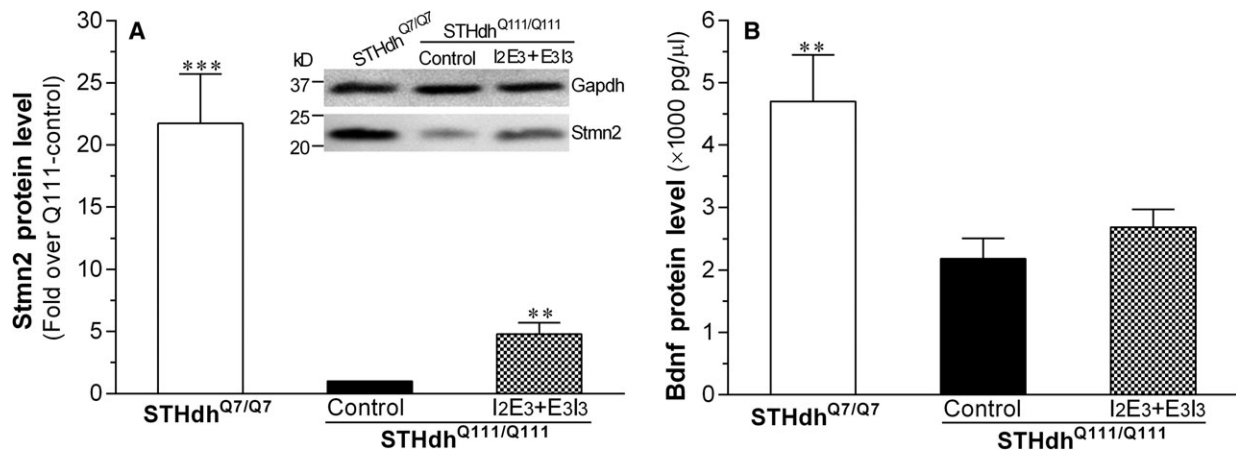


**Fig. 4** Comparison of *Stmn2* (A) and *Bdnf* (B) protein expression between STHdh<sup>Q7/Q7</sup> and STHdh<sup>Q111/Q111</sup> cells with or without ASOs treatment. Western blotting and ELISA were performed to assay protein expression of *Stmn2* and *Bdnf*, respectively. A representative Western blot for *Stmn2* with *Gapdh* as a loading control was shown as an inset. Data are shown as Mean ± S.E.M. ( $n = 3$ ). \*\* $P < 0.01$ , \*\*\* $P < 0.001$  compared with STHdh<sup>Q111/Q111</sup> control by Student's *t*-test.

influenced by the two approaches. For this reason, and considering the potential absence of correlation between expression levels of mRNA and protein [30], the effects of  $\Delta E_3$  induction and RNAi on Rest target gene transcription may not be simply determined by the observed alteration in Rest expression. However, based on the  $\Delta E_3$ -dependent effects of the ASOs on specific gene transcription (Fig. 3), a threshold along with a plateau likely exists for the transcriptional response to down-regulation of Rest function. Presumably, once the plateau (*i.e.* maximum derepression) is achieved, further down-regulation of Rest function will no longer increase transcriptional response, such may explain our observation of a similar transcriptional change yielded by  $\Delta E_3$  induction and RNAi regardless of the differed downregulation of REST by the two approaches.

Although reduced BDNF expression has been documented in HD [31], it was reported that BDNF levels in human blood are not informative nor reliable as HD biomarkers [32]. In accordance, we found that transcription of *Stmn2* and *Syn1*, but not *Bdnf*, was quite vulnerable to altered REST activity (*i.e.* up-regulation by mHtt and downregulation by ASOs/siRNA), suggesting that *Stmn2* and *Syn1* may have advantage over *Bdnf* as potential HD biomarkers. *Syn1* controls synapse function which is dysregulated in HD [33,34], with abnormal phosphorylation of *Syn1* being implicated in neurotransmission impairment in R6/2 HD mice [35]. By identifying a REST-controlled *Syn1*-S isoform predictive of loss-of-function, this study provides a new mechanism underlying synapse dysfunction in HD. As alternative splicing is epigenetically regulated while REST orchestrates cellular epigenome, it is not surprising that pre-mRNA splicing of *Syn1* (and probably other genes) is modulated by REST. *Stmn2* functions in microtubule stability and neuronal growth, and given that decreased *Stmn2* expression has been implicated in injury-induced axonal degeneration [36], Down's syndrome [37], and AD [38], the striking repression of *Stmn2* in HD cells suggests a common *Stmn2* dysfunction in a certain number of neurodegenerative diseases.

Besides *Bdnf*, *Stmn2* and *Syn1*, transcriptional profiling revealed ASOs-induced derepression of other genes in STHdh<sup>Q111/Q111</sup> cells. Despite the limited sample size, reliability of the transcriptional data was supported by several lines of evidence: (1) It is in good consistence with qRT-PCR data for the tested genes; (2) bioinformatics indicates that almost all the transcriptionally regulated genes harbour at least one RE-1 element; and (3) majority of the transcriptionally regulated genes are reportedly modulated by REST [39–41] and have been implicated in neurodegenerative diseases. For example, *Sarm1* and *Nmnat2* contribute to axonal degeneration—a critical, early event in neurodegenerative diseases [42,43], while *Unc13a*, *Vgf*, *Rtn2*, *Lrp11* and *Rundc3a* have been implicated in amyotrophic lateral sclerosis [44], frontotemporal dementia [45], hereditary spastic paraplegias [46], and Parkinson's disease and AD [47–49]. Thus, dysfunction of numerous specific genes is shared by neurodegenerative diseases, which may be explained by common pathogenic processes (*e.g.* axonal degeneration, endoplasmic reticulum stress and apoptosis) in such diseases. It should be pointed out that while only three samples were transcriptionally profiled, just a single dose and treatment duration of ASOs was examined in this study, making it possible that transcriptional regulation of some REST target genes cannot be observed in this study. Nevertheless, we demonstrate that repression of specific neuronal genes in STHdh<sup>Q111/Q111</sup>, which is presumably caused by mHtt-induced excessive nuclear REST, can be rescued by ASOs-induced  $\Delta E_3$  which reduces nuclear REST.

While increased nuclear REST and its neurotoxicity in HD were well documented [8–10] and supported by this study, Lu *et al.* [7] recently reported reduced nuclear REST in AD and neuroprotection of REST in ageing brain. This discrepancy may reflect the complexity of REST function under distinct pathophysiological conditions; however, considering the extensive alternative REST splicing, variable assays of REST might be attributable. Of the 45 REST mRNA variants we



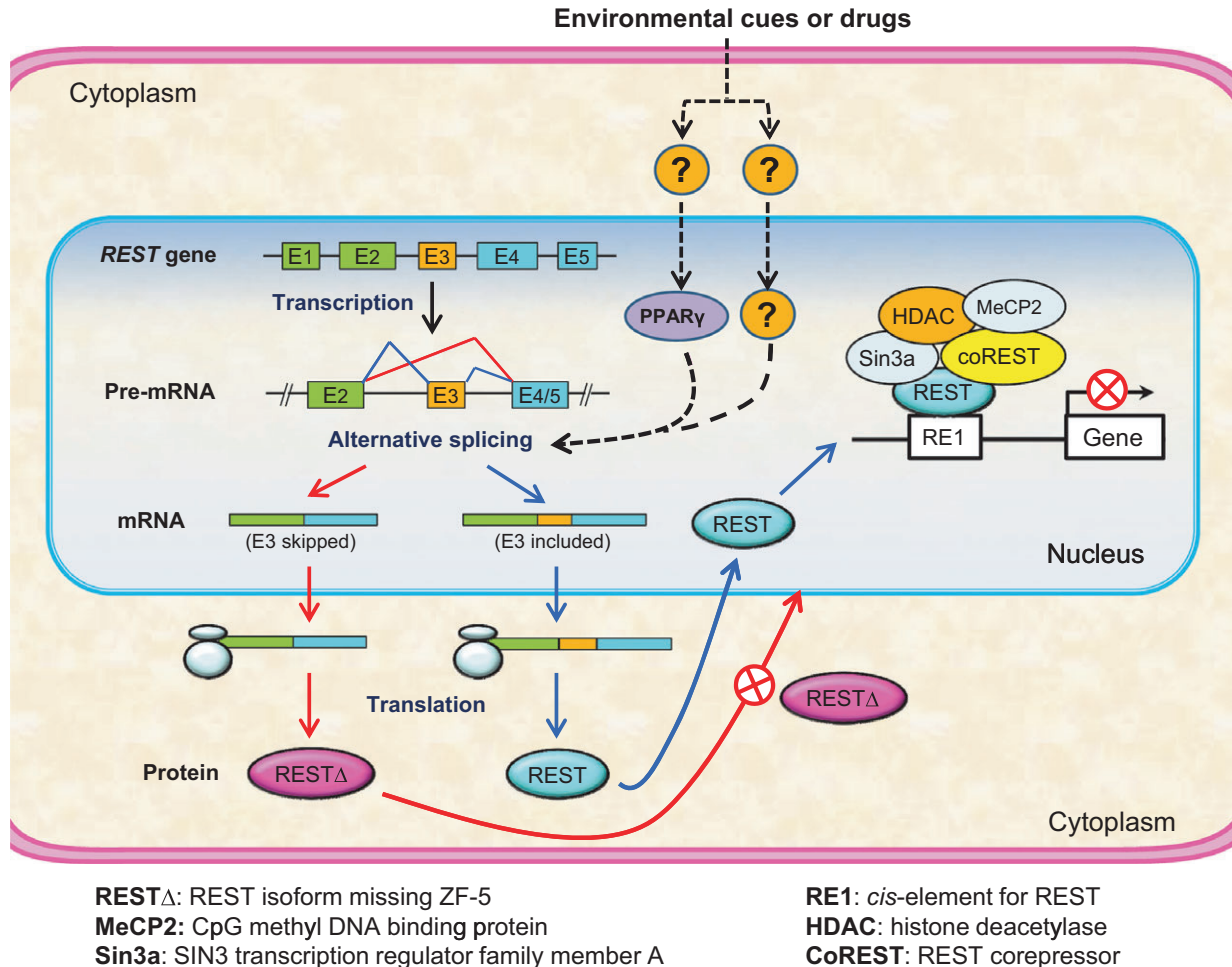


**Fig. 5** Illustration of  $\Delta E_3$  as an endogenous, manipulable modulator of REST function. The splicing event  $\Delta E_3$ , which is common in human and non-human primates, results in REST $\Delta$  protein isoform(s) missing ZF-5 critical for nuclear targeting and therefore modulates nuclear REST levels and genome function. Note that (1)  $\Delta E_3$  is modulated by PPAR $\gamma$  in a cell-dependent manner, presumably through a *cis*-element in E3; and (2) inclusion of E<sub>5</sub> as the last exon, which is mutually exclusive to E<sub>4</sub>, was only observed in human but not rodents and non-human primates [14].

previously identified, many are predictive of truncated protein products, of which REST4 is predicted by multiple mRNA variants [14], just like the case in rat [50]. Notably, it is recently reported that (1) for E<sub>2</sub>-lacking variants (e.g. E<sub>1a</sub>/E<sub>3</sub>/E<sub>4</sub>), an in-frame AUG in E<sub>3</sub> may initiate translation of a C-terminal REST<sup>C</sup> isoform (XP\_005265817) [51]; and (2) previously annotated noncoding RNAs with short ORF can encode small peptides [52,53], such might be the case for numerous REST variants (e.g. JX896962, JX896965 and JX896967). Hence, REST protein isoforms might be much more complex than we expected; however, not all the predicted REST protein isoforms have been experimentally verified, and due to post-translational modifications, they may not be observed as the predicted size by Western, making it challenging to determine whether an unexpected immunoreactive band is non-specific or a REST isoform. Due to the extensive alternative REST splicing, it can be inferred that assay of

REST by different primers/probes and antibodies may target different REST isoforms and therefore yield variable results. In support of this notion, the two anti-REST antibodies used in this study yielded distinct immunostaining profiles (Fig. 2 and Fig. S1) and different immunoreactive bands in accordance with the manufacturer's instruction (data not shown). In the study of Lu *et al.* [7], only the full-length REST was actually considered; however, qRT-PCR with four primer sets targeting different exons of REST yielded different expression levels, providing evidence for the existence of alternative REST splicing [54]. Notably, Lu *et al.* performed immunostaining with multiple anti-REST antibodies without considering differences between the antibodies and disclosing detailed usage of the antibodies, making it possible that nuclear REST differences between the experimental groups might be confounded by biased usage of the antibodies for samples of different groups [54].

In summary, using specific ASO<sub>3</sub> which induces a common alternative splicing ( $\Delta E_3$ ), we demonstrate that  $\Delta E_3$  modulates nuclear REST and its gene regulation function in a cellular module of HD, and it thus represents a potential therapeutic target for HD. Our findings, which may extend to *in vivo* due to the ASOs-induced  $\Delta E_3$  in mouse primary neurons, highlight the role of alternative splicing in modulation of REST function and provide new insights into environmental regulation of genome function as well as the pathogenesis of HD.

## Acknowledgements

This work was supported by NIH grants DA030177 (GMM) and DA025697 (GMM). We thank Hong Yang and Lisa Ogawa for their technical support. We are grateful to Professor Bertha Mardras at the Department of Psychiatry, Harvard Medical School for her helpful suggestions. We thanks Liying Liu and Matthew Poulin from Epigendx Inc for their assistance for data analysis.

## References

- Ooi L, Wood IC. Chromatin crosstalk in development and disease: lessons from REST. *Nat Rev Genet.* 2007; 8: 544–54.
- Bithell A. REST: transcriptional and epigenetic regulator. *Epigenomics.* 2011; 3: 47–58.
- Qureshi IA, Gokhan S, Mehler MF. REST and CoREST are transcriptional and epigenetic regulators of seminal neural fate decisions. *Cell Cycle.* 2010; 9: 4477–86.
- Shimojo M. Characterization of the nuclear targeting signal of REST/NRSF. *Neurosci Lett.* 2006; 398: 161–6.
- Shimojo M, Lee JH, Hersh LB. Role of zinc finger domains of the transcription factor neuron-restrictive silencer factor/repressor element-1 silencing transcription factor in DNA binding and nuclear localization. *J Biol Chem.* 2001; 276: 13121–6.
- Guan H, Ricciardi RP. Transformation by E1A oncoprotein involves ubiquitin-mediated proteolysis of the neuronal and tumor repressor REST in the nucleus. *J Virol.* 2012; 86: 5594–602.
- Lu T, Aron L, Zullo J, et al. REST and stress resistance in ageing and Alzheimer's disease. *Nature.* 2014; 507: 448–54.
- Buckley NJ, Johnson R, Zuccato C, et al. The role of REST in transcriptional and epigenetic dysregulation in Huntington's disease. *Neurobiol Dis.* 2010; 39: 28–39.
- Zuccato C, Tartari M, Crotti A, et al. Huntingtin interacts with REST/NRSF to modulate the transcription of NRSE-controlled neuronal genes. *Nat Genet.* 2003; 35: 76–83.
- Zuccato C, Belyaev N, Conforti P, et al. Widespread disruption of repressor element-1 silencing transcription factor/neuron-restrictive silencer factor occupancy at its target genes in Huntington's disease. *J Neurosci.* 2007; 27: 6972–83.
- Soldati C, Bithell A, Conforti P, et al. Rescue of gene expression by modified REST decoy oligonucleotides in a cellular model of Huntington's disease. *J Neurochem.* 2011; 116: 415–25.
- Conforti P, Mas Monteys A, Zuccato C, et al. *In vivo* delivery of DN:REST improves transcriptional changes of REST-regulated genes in HD mice. *Gene Ther.* 2013; 20: 678–85.
- Westbrook TF, Hu G, Ang XLL, et al. SCF beta-TRCP controls oncogenic transformation and neural differentiation through REST degradation. *Nature.* 2008; 452: 370–4.
- Chen G-L, Miller GM. Extensive alternative splicing of the repressor element silencing transcription factor linked to cancer. *PLoS One.* 2013; 8: e62217.
- Bordet R, Ouk T, Petraut O, et al. PPAR: a new pharmacological target for neuroprotection in stroke and neurodegenerative diseases. *Biochem Soc Trans.* 2006; 34: 1341–6.
- Rosen ED, Spiegelman BM. PPAR $\gamma$ : a nuclear regulator of metabolism, differentiation, and cell growth. *J Biol Chem.* 2001; 276: 37731–4.
- Murphy GJ, Holder JC. PPAR- $\gamma$  agonists: therapeutic role in diabetes, inflammation and cancer. *Trends Pharmacol Sci.* 2000; 21: 469–74.
- Ghose J, Sinha M, Das E, et al. Regulation of miR-146a by RelA/NF $\kappa$ B and p53 in STHdh(Q111)/Hdh(Q111) cells, a cell model of Huntington's disease. *PLoS One.* 2011; 6: e23837.
- Gines S, Ivanova E, Seong IS, et al. Enhanced Akt signaling is an early pro-survival response that reflects N-methyl-D-aspartate receptor activation in Huntington's disease knock-in striatal cells. *J Biol Chem.* 2003; 278: 50514–22.
- Lee JM, Ivanova EV, Seong IS, et al. Unbiased gene expression analysis implicates the huntingtin polyglutamine tract in extra-mitochondrial energy metabolism. *PLoS Genet.* 2007; 3: e135.
- Trettel F, Rigamonti D, Hilditch-Maguire P, et al. Dominant phenotypes produced by the HD mutation in STHdhQ111 striatal cells. *Hum Mol Genet.* 2000; 9: 2799–809.
- Livak KJ, Schmittgen TD. Analysis of relative gene expression data using real-time quantitative PCR and the 2 $^{-\Delta\Delta CT}$  method. *Methods.* 2001; 25: 402–8.
- Alló M, Schor IE, Muñoz MJ, et al. Chromatin and alternative splicing. *Cold Spring Harb Symp Quant Biol.* 2010; 75: 103–11.
- Schwartz S, Meshorer E, Ast G. Chromatin organization marks exon-intron structure. *Nat Struct Mol Biol.* 2009; 16: 990–5.
- Raj B, O'Hanlon D, Vessey JP, et al. Cross-regulation between an alternative splicing activator and a transcription repressor controls neurogenesis. *Mol Cell.* 2011; 43: 843–50.
- Douglas AG, Wood MJ. Splicing therapy for neuromuscular disease. *Mol Cell Neurosci.* 2013; 56: 169–85.
- Kole R, Krainer AR, Altman S. RNA therapeutics: beyond RNA interference and antisense oligonucleotides. *Nat Rev Drug Discovery.* 2012; 11: 125–40.

## Conflict of interest

All of the authors do not have any financial disclosures to report.

## Supporting information

Additional Supporting Information may be found online in the supporting information tab for this article:

**Fig. S1** The effect of ASOs on  $\Delta E_3$  in additional cells (A) and nuclear REST in RN46A cells (B).

**Fig. S2** Expanded view of immunofluorescence analysis of STHdh<sup>Q71</sup> and STHdh<sup>Q111/Q111</sup> cells with/-out ASOs treatment.

28. **Osman EY, Miller MR, Robbins KL, et al.** Morpholino antisense oligonucleotides targeting intronic repressor Element1 improve phenotype in SMA mouse models. *Hum Mol Genet.* 2014; 23: 4832–45.
29. **Azoulay L, Yin H, Filion KB, et al.** The use of pioglitazone and the risk of bladder cancer in people with type 2 diabetes: nested case-control study. *BMJ.* 2012; 344.
30. **de Sousa Abreu R, Penalva LO, Marcotte EM, et al.** Global signatures of protein and mRNA expression levels. *Mol BioSyst.* 2009; 5: 1512–26.
31. **Zuccato C, Cattaneo E.** Role of brain-derived neurotrophic factor in Huntington's disease. *Prog Neurobiol.* 2007; 81: 294–330.
32. **Zuccato C, Marullo M, Vitali B, et al.** Brain-derived neurotrophic factor in patients with Huntington's disease. *PLoS One.* 2011; 6: e22966.
33. **Cesca F, Baldelli P, Valtorta F, et al.** The synapsins: key actors of synapse function and plasticity. *Prog Neurobiol.* 2010; 91: 313–48.
34. **Smith R, Brundin P, Li JY.** Synaptic dysfunction in Huntington's disease: a new perspective. *Cell Mol Life Sci.* 2005; 62: 1901–12.
35. **Lievens JC, Woodman B, Mahal A, et al.** Abnormal phosphorylation of synapsin I predicts a neuronal transmission impairment in the R6/2 Huntington's disease transgenic mice. *Mol Cell Neurosci.* 2002; 20: 638–48.
36. **Shin JE, Miller BR, Babetto E, et al.** SCG10 is a JNK target in the axonal degeneration pathway. *Proc Natl Acad Sci U S A.* 2012; 109: E3696–705.
37. **Bahn S, Mimmack M, Ryan M, et al.** Neuronal target genes of the neuron-restrictive silencer factor in neurospheres derived from fetuses with Down's syndrome: a gene expression study. *Lancet (London, England).* 2002; 359: 310–5.
38. **Okazaki T, Wang H, Masliah E, et al.** SCG10, a neuron-specific growth-associated protein in Alzheimer's disease. *Neurobiol Aging.* 1995; 16: 883–94.
39. **Wagoner MP, Gunsalus KTW, Schoenike B, et al.** The transcription factor REST is lost in aggressive breast cancer. *PLoS Genet.* 2010; 6: e1000979.
40. **Sedaghat Y, Bui HH, Mazur C, et al.** Identification of REST-regulated genes and pathways using a REST-targeted antisense approach. *Nucleic Acid Ther.* 2013; 23: 389–400.
41. **Moon SM, Kim JS, Park BR, et al.** Transcriptional regulation of the neuropeptide VGF by the neuron-restrictive silencer factor/neuron-restrictive silencer element. *NeuroReport.* 2015; 26: 144–51.
42. **Gilley J, Orsomando G, Nascimento-Ferreira I, et al.** Absence of SARM1 rescues development and survival of NMNAT2-deficient axons. *Cell Rep.* 2015; 10: 1974–81.
43. **Gerdts J, Brace EJ, Sasaki Y, et al.** SARM1 activation triggers axon degeneration locally via NAD(+) destruction. *Science.* 2015; 348: 453–7.
44. **Vidal-Taboada JM, Lopez-Lopez A, Salvado M, et al.** UNC13A confers risk for sporadic ALS and influences survival in a Spanish cohort. *J Neurol.* 2015; 262: 2285–92.
45. **Gijssels I, van der Zee J, Engelborghs S, et al.** Progranulin locus deletion in frontotemporal dementia. *Hum Mutat.* 2008; 29: 53–8.
46. **Montenegro G, Rebelo AP, Connell J, et al.** Mutations in the ER-shaping protein reticulon 2 cause the axon-degenerative disorder hereditary spastic paraplegia type 12. *J Clin Invest.* 2012; 122: 538–44.
47. **Cocco C, D'Amato F, Noli B, et al.** Distribution of VGF peptides in the human cortex and their selective changes in Parkinson's and Alzheimer's diseases. *J Anat.* 2010; 217: 683–93.
48. **Marks N, Berg MJ.** Neurosecretases provide strategies to treat sporadic and familial Alzheimer disorders. *Neurochem Int.* 2008; 52: 184–215.
49. **Offe K, Dodson SE, Shoemaker JT, et al.** The lipoprotein receptor LR11 regulates amyloid beta production and amyloid precursor protein traffic in endosomal compartments. *J Neurosci.* 2006; 26: 1596–603.
50. **Palm K, Belluardo N, Metsis M, et al.** Neuronal expression of zinc finger transcription factor REST/NRSF/XRB gene. *J Neurosci.* 1998; 18: 1280–96.
51. **Nechiporuk T, McGann J, Mullendorff K, et al.** The REST remodeling complex protects genomic integrity during embryonic neurogenesis. *eLife.* 2016; 5: e09584. <http://dx.doi.org/10.7554/eLife.09584>
52. **Magny EG, Pueyo JI, Pearl FMG, et al.** Conserved regulation of cardiac calcium uptake by peptides encoded in small open reading frames. *Science.* 2013; 341: 1116–20.
53. **Nelson BR, Makarewich CA, Anderson DM, et al.** A peptide encoded by a transcript annotated as long noncoding RNA enhances SERCA activity in muscle. *Science.* 2016; 351: 271–5.
54. **Chen G-L, Miller GM.** Alternative REST splicing underappreciated. *bioRxiv.* 2017. DOI: <https://doi.org/10.1101/119552>.